

A REPORT ON
Path Tracking Control of Autonomous Ground Vehicle (AGV)

By
B Sai Venkatesh
ID: 2018A4PS0346H

Prepared in partial fulfilment of the
Practice School-II Course No. BITS C413

At
Centre for Artificial Intelligence and Robotics (CAIR), DRDO, Bangalore,
India
A Practice School-II Station of

BIRLA INSTITUTE OF TECHNOLOGY AND SCIENCE, PILANI (Hyderabad)



Jul 2021 -Dec 2021

ACKNOWLEDGEMENT

This project would not have been possible without the kind support and help of many individuals. I would like to extend my sincere thanks to all of them.

I am thankful to Dr. Shubhashisa Sahoo for giving me the golden opportunity to work on this project. I am highly indebted to the members of the ISRD Division at, Centre for Artificial Intelligence and Robotics, Bangalore, India for their guidance and constant supervision. I am also thankful to Mr. Pradeep Sharma for providing me with the necessary support during my internship. Last but not the least, I am extremely thankful to the Practice School Division, BITS Pilani and my instructor Prof. S Raghuraman for helping me find an internship opportunity at Centre for Artificial Intelligence and Robotics, Bangalore.

Practice School Division

Station Name: Centre for Artificial Intelligence and Robotics (CAIR), DRDO

Centre: Bangalore

Duration: 5 months

Date of Start: 26th July 2021

Date of Report Submission: 13th December 2021

Title of the Project: Path Tracking Control of Autonomous Ground Vehicle (AGV)

Name: B Sai Venkatesh

ID No: 2018A4PS0346H

Discipline of Student: Mechanical Engineering

Name and Designation of the Expert: Dr. Subhashisa Sahoo, Scientist F

Name of the PS Faculty: Prof. S. Raghuraman

Key words: Path tracking, Sliding mode control, Control systems, Autonomous driving, Model Predictive Control

Project Areas: Control Systems, Vehicle Dynamics

ABSTRACT

In the recent years, a spike in the demand for Autonomous Ground Vehicles (AGVs) has generated considerable interest in the navigation of AGVs. A significant task in navigation is the design of path trackers, which help in guiding the vehicle along the path prescribed by the path planner. This is a challenging task as it depends on the vehicle parameters, the terrain conditions, and the dynamics of the steering actuator as well.

The dynamics of the vehicle are modelled using the bicycle model that considers the ground-wheel and side-slip angle. A Robust Adaptive Sliding Mode Controller (RASMC) and Model Predictive Controller (MPC) are used for the heading angle controller and the controller performance is evaluated on a Lane Change maneuver under constant longitudinal speed. The controller is designed on the MATLAB-Simulink platform and co-simulated with CarSim under a variety of speeds.

In simulation, it is observed that in RASMC and MPC, when the vehicle is moving at 10 m/s, a heading angle change of 10° can be achieved within 3 seconds in the presence of disturbances. It is also observed that RASMC and MPC give similar results under the presence and absence of disturbances.

Contents

ABSTRACT	4
List of Figures and Tables	6
Nomenclature	7
Chapter 1: Introduction	8
Chapter 2: Vehicle Dynamics and Steering Actuator	10
2.1: Vehicle Dynamics	10
2.2: Steering Actuator	14
Chapter 3: Robust Adaptive Sliding Mode Controller	17
3.1: Introduction to Robust Adaptive Sliding Mode Controller	17
3.2: Implementation	18
Chapter 4: Model Predictive Control	21
4.1: Introduction to Model Predictive Control	21
4.2: Implementation	22
Chapter 5: Results	23
References	25

List of Figures and Tables

Figure 1: Bicycle model representing vehicle dynamics

Figure 2: Tire slip-angle

Figure 3: Actuator Model

Figure 4: Total System of Heading Angle Controller

Figure 5: Structure of the system and the heading angle controller

Figure 6: Simulink Diagram of Robust Adaptive Sliding Mode Controller

Figure 7: SMC Subsystem

Figure 8: Disturbance estimator subsystem

Figure 9: Model Predictive Controller

Figure 10: Steering Wheel Angle and Yaw of the AGV at 5 m/s with RASMC

Figure 11: Yaw of the AGV at 5 m/s with MPC

Figure 12: Steering Wheel Angle and Yaw of the AGV at 10 m/s with RASMC

Figure 13: Yaw of the AGV at 10 m/s with MPC

Table 1: Values of Vehicle Parameters

Table 2: Values of Steering Actuator Parameters

Nomenclature

b – Viscous Friction Coefficient

C_f – Cornering stiffness for the front wheel

C_r – Cornering stiffness for the rear wheel

F_{yf} – Lateral tire force on the front wheel

F_{yr} – Lateral tire force on the rear wheel

I_z – Yaw moment of inertia of the vehicle

J – Rotor Inertia

K_b – Back emf constant

K_t – Torque Constant

l – Wheelbase

L – Terminal Inductance

l_f – Distance of the front tire from vehicle CG

l_r – Distance of the rear tire from vehicle CG

m – Mass of the vehicle

N – Nominal Speed

r – Yaw rate of the vehicle

R – Terminal Resistance

T – Nominal Torque

v – Velocity of the vehicle

V – Nominal Voltage

w – Track width

δ – Steering angle of the front wheel

θ – Vehicle yaw angle measured w.r.t global X-axis

φ – Steering Shaft Rotation

Chapter 1: Introduction

Autonomous Ground Vehicles (AGVs) are intelligent vehicles that function without the assistance of a human operator. They usually have a variety of sensors to sense the environment and navigate based on the information they gather. It is capable of making decisions on its own without the need for human intervention. As a result, AGVs can be utilized in various dangerous applications, such as military applications, bomb detection, and mining, while reducing human exposure to these threats [1]-[5].

AGVs can detect obstacles and navigate around them to reach a goal point. It has a localization subsystem consisting of an Inertial Measurement Unit (IMU), odometer, compass, and GPS that measures the position, orientation, velocity, and yaw rate. The design of path trackers, which assist in steering the vehicle along the course given by the path planner, is an important challenge in navigation because it is dependent on vehicle factors, terrain conditions, and the steering actuator's dynamics.

In [6] and [7], the path tracking controllers based on the Sliding Mode Controller (SMC) are proposed. The results show that the SMC can make the vehicle track its path satisfactorily and smoothly. [8], [9] uses a Non-Singular Terminal Sliding Mode (NSTM) control to ensure that the SMC can converge in a limited time, and reduce the vibration of the controller caused by switching motion of the sliding surface. In addition, [10] proposed a novel approach which integrates the backstepping technique and adaptive sliding mode control for the automatic steering control of AGVs and a good robustness against vehicular velocity and tracking accuracy is achieved.

Because of its ability to handle complex constraints, Model Predictive Controller (MPC) has been widely used in the automotive industry [11]. Considering that the vehicle is subject to kinematic constraints, dynamic constraints, and actuator constraints, [12] and [13] use the Model Predictive Control (MPC) to achieve the trajectory following control. In [14], an optimal tracking MPC while avoiding collision with obstacles has been formulated. [15] uses MPC to improve vehicle yaw stability, when braking forces are applied to the wheels to constrain yaw moments. In [16], a regional path tracking problem of AGV has been discussed based on MPC, with the front wheel steering angle as the control variable, and the safety and actuator constraints factors were also considered.

This report focuses primarily on the path tracking aspect of the Autonomous Ground Vehicle. It is done by using a Robust Adaptive Sliding Mode Controller (RASMC) and a Model Predictive Controller (MPC). The vehicle dynamics are modelled using a single-track car model popularly known as Bicycle Model [17]. The controller is tested under a variety of terrains and environments and the controller performance is evaluated. The dynamics of the vehicle and steering actuator is discussed in chapter 2. The controllers used for path tracking is discussed in chapters 3 and 4. The results and concluding remarks are provided in chapter 5.

Chapter 2: Vehicle Dynamics and Steering Actuator

2.1: Vehicle Dynamics

The test vehicle has an Ackermann like steering mechanism and only the front wheels are steerable. A single-track car model popularly known as the “bicycle model” [8] is selected to represent the dynamics of the test vehicle. The “single-track car model” has two degrees of freedom and it is the simple approximation to the lateral dynamics of an Ackerman steered wheeled vehicle. It also assumes uniform mass distribution in the right and left sides of the vehicle and combines the effect of two wheels on the same axle and treats them as a single wheel positioned between the two wheels.

The vehicle parameters of the AGV are derived from a commercially available 4 wheeled battery-operated vehicle, the CARRIEALL car as described in [18]. The steering wheel is driven by a DC motor with a 156:1 gear ratio. The parameter values considered for the test vehicle are given below in Table 1.

Parameter	Value	Unit
Mass at front-left wheel (m_{fl})	158	kg
Mass at front-right wheel (m_{fr})	137	kg
Mass at rear-left wheel (m_{rl})	360	kg
Mass at rear-right wheel (m_{rr})	269	kg
Mass of the vehicle (m)	924	kg
Wheelbase (l)	1.93	m
Location of CG from front axle (l_f)	1.31	m
Location of CG from rear axle (l_r)	0.62	m
Moment of Inertia (I_z)	932	kgm ²

Table 1: Values of Parameters based on [19]

In control system design, a linearized model is frequently sufficient to offer satisfactory performance in the operating range of interest. A linear and time invariant (LTI) model is used in most land vehicle control applications. A bicycle model of the vehicle with two degrees of freedom is considered. The two degrees of freedom are represented by the vehicle lateral position, y , and the vehicle yaw angle, θ .

Consider v_x to be the longitudinal velocity of the vehicle, v_y to be the lateral velocity of the vehicle, and r to be the yaw rate of the vehicle. The equation for the lateral motion of the vehicle can be given by,

$$\mathbf{a} = (\dot{v}_x - v_y r)\mathbf{i} + (\dot{v}_y + v_x r)\mathbf{j} \quad (1)$$

Using equation (1), we get the longitudinal and lateral acceleration. Considering m as the mass of the vehicle, I_z as the yaw moment of inertia, F_{yf} and F_{yr} as the lateral force on the rear tyre respectively, δ as the steering angle, we get

$$m(\dot{v}_y(t) + v_x(t)r(t)) = F_{xf} \sin \delta(t) + F_{yf} \cos \delta(t) + F_{yr}(t) \quad (2)$$

The equation governing the yaw motion is given by

$$I_z \dot{r}(t) = l_f F_{xf} \sin \delta(t) + l_f F_{yf} \cos \delta(t) - l_r F_{yr}(t) \quad (3)$$

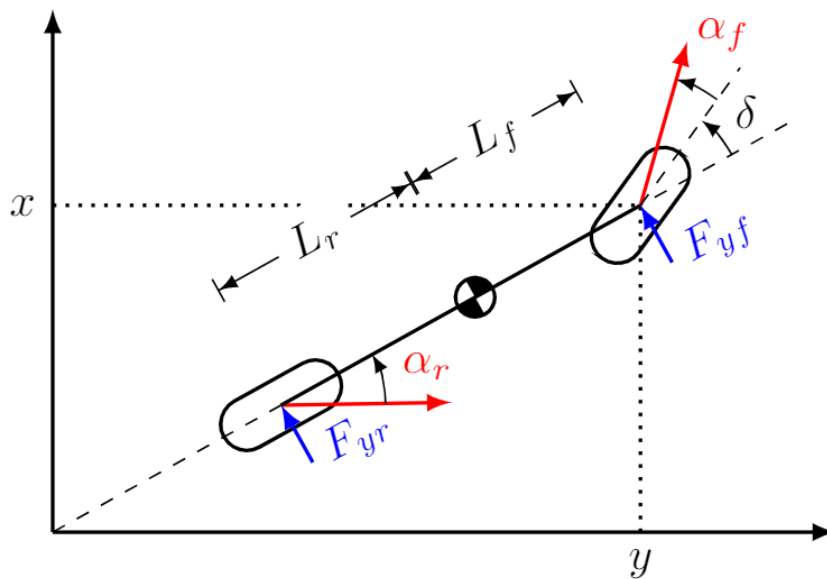


Figure 1: Bicycle model representing vehicle dynamics

Considering the steering angle, δ to be small, we can rewrite equations (2) and (3) as follows

$$m(\dot{v}_y(t) + v_x(t)r(t)) = F_{yf}(t) + F_{yr}(t)$$

$$I_z \dot{r}(t) = l_f F_{yf}(t) - l_r F_{yr}(t) \quad (4)$$

The slip angle is the angle between the orientation of the tyre and the direction of the velocity vector at the tyre. For small slip angles, the lateral tyre force is proportional to the slip angle. The lateral forces acting on front and rear wheels are represented are given by

$$F_{yf}(t) = C_f \alpha_f(t) \text{ and } F_{yr}(t) = C_r \alpha_r(t) \quad (5)$$

where α_f is the slip angle of the front wheel and α_r slip angle of the rear wheel. C_f and C_r are the cornering stiffness of the front tyre and the cornering stiffness of the rear tyre, respectively. The sideslip angles for both the front and rear tyres are described as given in figure 3.

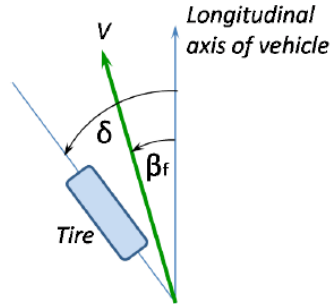


Figure 2: Tire slip-angle

$$\tan \beta_f = \frac{v_y + l_f r}{v_x} \text{ or } \beta_f \approx \frac{v_y + l_f r}{v_x} \quad (6)$$

$$\tan \beta_r = \frac{v_y - l_r r}{v_x} \text{ or } \beta_r \approx \frac{v_y - l_r r}{v_x} \quad (7)$$

Assuming β_f is small, we have,

$$\alpha_f(t) = \delta(t) - \beta_f \text{ and } \alpha_r(t) = -\beta_r \quad (8)$$

This implies,

$$\alpha_f(t) = \delta(t) - \left(\frac{v_y + l_f r}{v_x} \right) \text{ and } \alpha_r(t) = - \left(\frac{v_y - l_f r}{v_x} \right) \quad (9)$$

Using the equations (5) and (9), the governing equation (4) is described as

$$m\dot{v}_y(t) + \left(\frac{C_f + C_r}{v_x} \right) v_y(t) + \left(m v_x + \frac{C_f l_f - C_r l_r}{v_x} \right) r(t) = C_f \delta(t) \quad (10)$$

and

$$I_z \dot{r}(t) + \left(\frac{C_f l_f - C_r l_r}{v_x} \right) v_y(t) + \left(\frac{C_f l_f^2 + C_r l_r^2}{v_x} \right) r(t) = C_f l_f \delta(t) \quad (11)$$

2.2: Steering Actuator

The steering wheels of the UGV should execute the command signals received from the vehicle controller and maintain coordination with the steering actuator in order to maintain the heading angle of the vehicle. The actuator dynamics and response time for obtaining the necessary steering angle were of the same order as the heading angle dynamics in the existing model. As a result, in order to create a system model that effectively predicts real-world system behaviour, it is vital to integrate steering actuator dynamics during modelling. The actuator used here is a DC motor whose transfer function is derived from the first principles. A closed loop proportional controller with a gain of $K_p = 2$ is used to control it. The feedback is given by the encoder that measures rotation of steering shaft and using gear ratio, the rotation of the front wheel. The steering angle parameters are listed in Table 2.

Parameter	Value	Unit
Terminal Resistance (R)	0.317	Ohms
Terminal Inductance (L)	0.0823	mH
Torque Constant (K_t)	30.2	mNm/A
Speed Constant	317	rpm/V
Back emf constant (K_b)	0.0301	V/rad/sec
Rotor Inertia (J)	138	g.cm ²
Speed / Torque Gradient	3.33	rpm/mNm
Nominal Speed (N)	6930	rpm
Nominal Torque (T)	170	mNm
Nominal Voltage (V)	24	V

Table 2: Values of parameters based on [19]

The Transfer function for the steering actuator is derived as,

$$\text{Torque Generated, } T = K_t i \quad (12)$$

$$\text{Back emf, } V_b = K_b \dot{\theta} \quad (13)$$

From Figure 3,

$$J\ddot{\theta} + b\dot{\theta} = K_t i \quad (14)$$

$$L \frac{di}{dt} + Ri = V - K_b \dot{\theta} \quad (15)$$

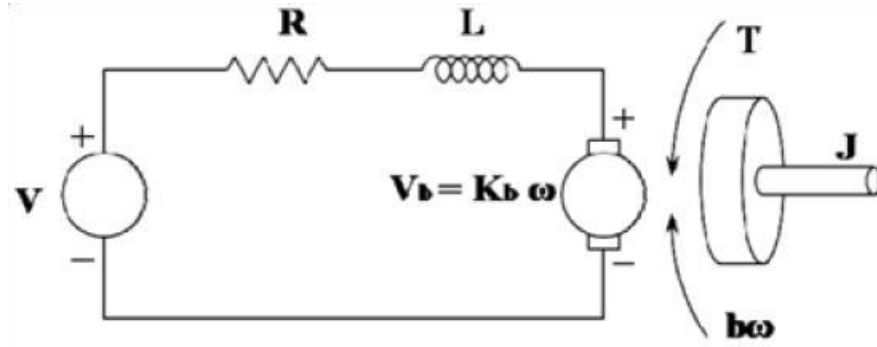


Figure 3: Actuator Model

Applying the Laplace transform to equations (14) and (15), we get

$$s(Js + b)\theta(s) = K_t I(s) \quad (16)$$

$$(Ls + R)I(s) = V(s) - K_b s\theta(s) \quad (17)$$

Simplifying equations (16) and (17), we get

$$\frac{\theta(s)}{I(s)} = \frac{K_t}{s(Js+b)} \quad (18)$$

$$\frac{\theta(s)}{V(s)} = \frac{K_t}{s[(Js+b)(Ls+R)+K_t K_b]} \quad (19)$$

$$G_V^\theta = \frac{K_t}{s[(Ls+R)(Js+b)+K_t K_b]} \quad (20)$$

K_t – Torque Constant
 L – Inductance
 R – Resistance
 J – Rotor Inertia
 b – Viscous Friction Coefficient
 V - Input Voltage to the motor
 φ – Steering Shaft Rotation

On substituting the values of these parameters from the data sheet of the motor (listed in table 2), and ignoring the higher order terms such as JLs^3 (because they are negligibly small in magnitude), we have

$$G_V^\varphi = \frac{302}{s(0.044s + 9.164)} \quad (21)$$

In practice, the front wheel can no longer turn more than ± 30 degrees. As a result, a saturation block is added to the input, limiting the maximum intended steering angle to ± 30 degrees. A saturation block also limits the maximum voltage that can be applied to the motor between ± 20 volts. This corresponds to the actuator's physical restrictions. Based on this, the steering controller is designed and it is represented in Figure 4.

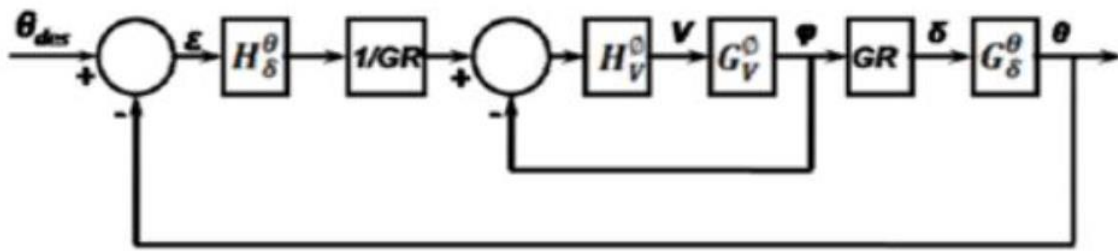


Figure 4: Total System of Heading Angle Controller [19]

Figure 4 consists of two control loops: an inner control loops that is responsible for the steering angle and an outer loop that is responsible for the heading angle. Together, they help the vehicle to move in the appropriate path given by the path planner.

Chapter 3: Robust Adaptive Sliding Mode Controller

3.1: Introduction to Robust Adaptive Sliding Mode Controller

Sliding Mode Control (SMC) is a robust control approach that may be used to govern both linear and nonlinear systems. SMC involves two modes of operations, viz., reaching mode and sliding mode [20]. The system trajectory travels towards the sliding surface (a user-defined surface with desired attributes) in reaching mode. When the trajectory collides with the sliding surface, it begins to slide down the surface in the direction of the equilibrium point, resulting in sliding mode motion. The invariance of the SMC technique to uncertainty and disruption in the sliding mode is its main advantage. SMC is a robust control method that may be employed for a wide range of practical control applications due to its invariance quality.

The control scheme considered here uses a Sliding Mode Controller with Power Rate Reaching Law (PRRL), a parameter estimator that is the adaptive part of the controller, and a perturbation estimator that estimates and compensates for disturbance. The system is very robust on account of its ability to deal with a large class of uncertainties like, uncertainties in model parameter estimation, unmodelled dynamics and external disturbances. The robustness to external disturbances is partly due to the SMC which is more robust on account of the new reaching law and partly due to the disturbance estimator that cancels out the external disturbances. Figure 5 shows the structure of the controller.

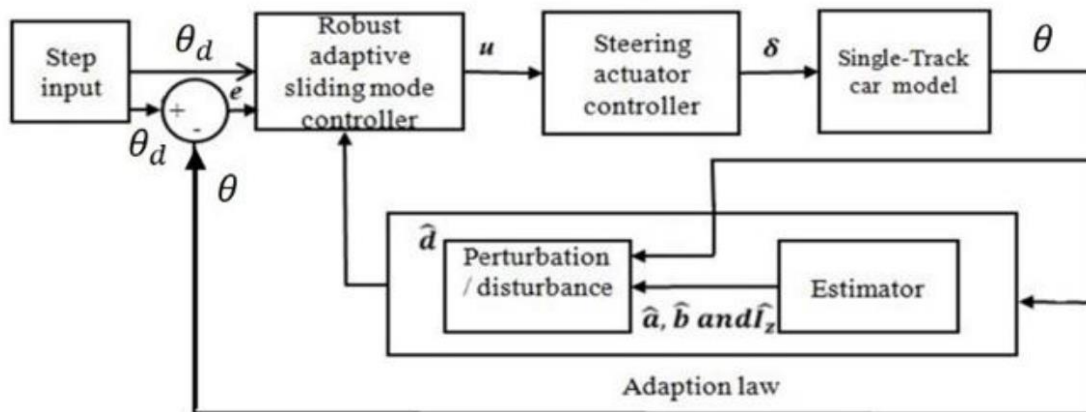


Figure 5: Structure of the system and the heading angle controller

For this robust adaptive sliding mode controller, the Power Rate Reaching Law (PRRL) is considered. It is given by,

$$\dot{s}(t) = -K_p |s|^\sigma \text{sign}(s), K_p > 0, 0 < \sigma < 1 \quad (22)$$

σ – Power Factor

K_p – Proportional Switching Constant

$$\text{sign}(s) \begin{cases} = 1, \text{ when } s = 1 \\ = 0, \text{ when } s = 0 \\ = -1, \text{ when } s = -1 \end{cases}$$

The Power Rate Reaching law (PRRL) is an improvement over the previously considered Constant reaching law consisting of the signum function, and the saturation function considered to reduce chattering.

3.2: Implementation

The controller is designed in MATLAB-Simulink and is given in Figure 6. The controller design can be divided into the following subdivisions – adaptive sliding mode controller, steering controller, parameter estimator and disturbance estimator. The adaptive sliding mode controller is designed in Figure 7. The adaptive sliding mode controller provides the required steering angle as output. This value is taken as input by the steering subsystem. The steering subsystem consists of a closed loop controller with $K_p = 2$ and the transfer function of the steering actuator modelled in (18). The disturbance estimator estimates the disturbance present based on the estimated parameters. It is designed in Figure 8. Overall, there are two control loops: the outer loop that is responsible for the heading angle control and an inner loop that is responsible for the steering angle. These control loops together provide the vehicle appropriate motion. We test the controller for a heading angle change of 10° .

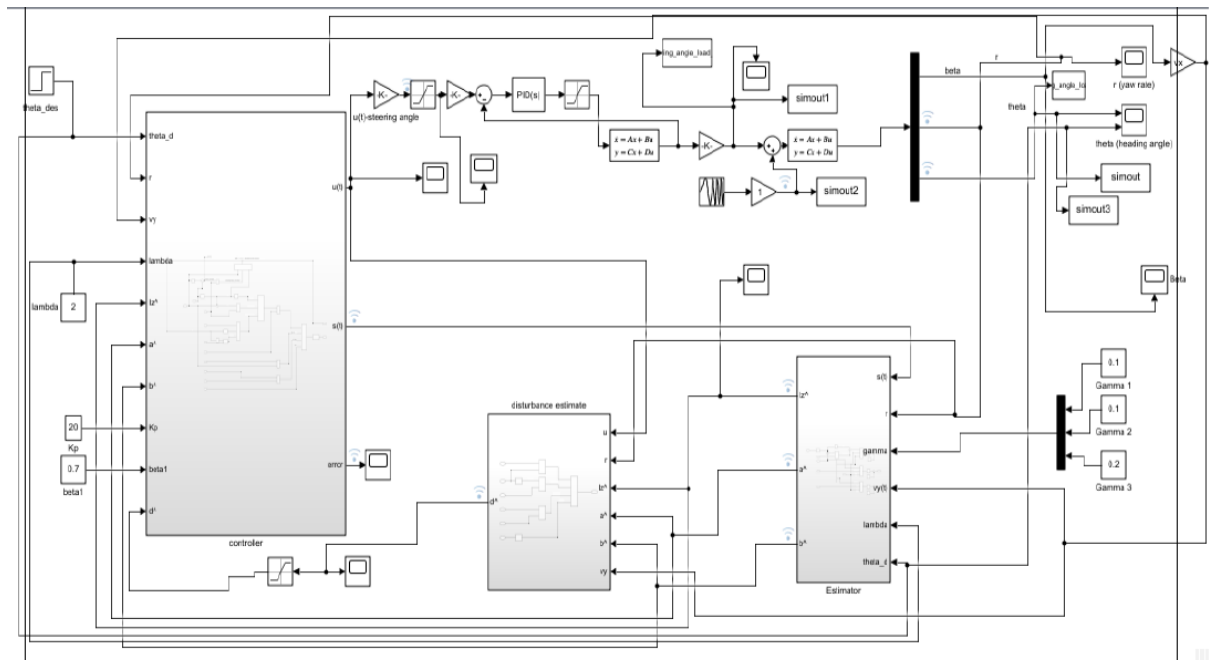


Figure 6: Simulink Diagram of Robust Adaptive Sliding Mode Controller

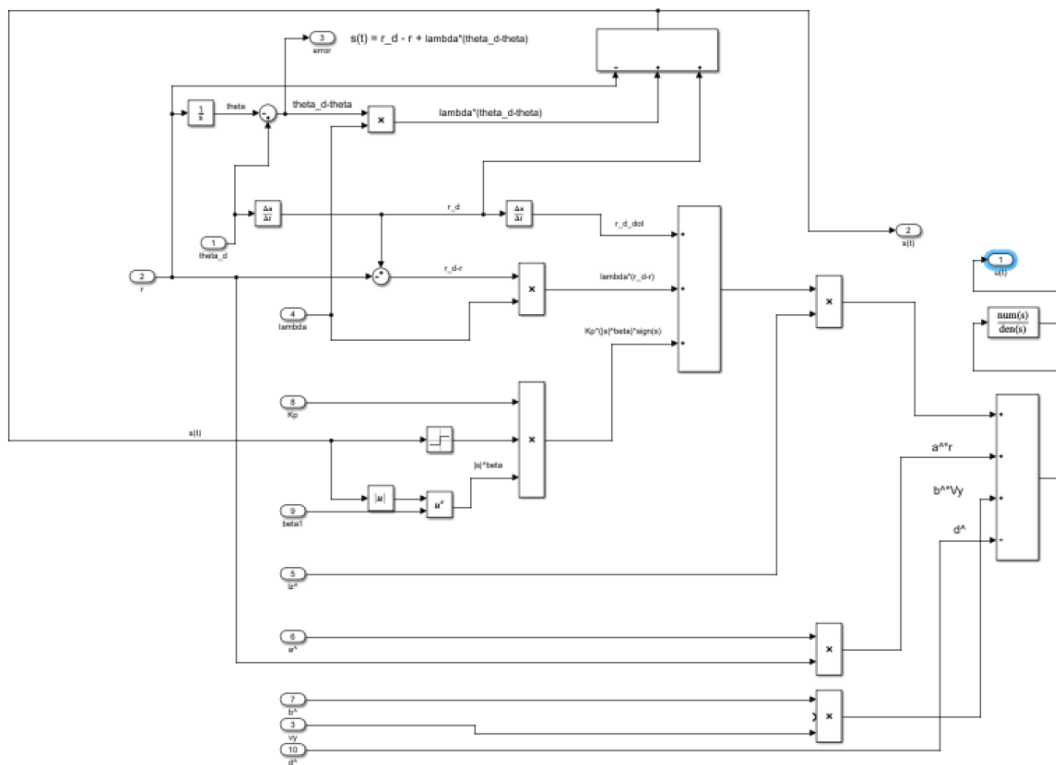


Figure 7: SMC Subsystem

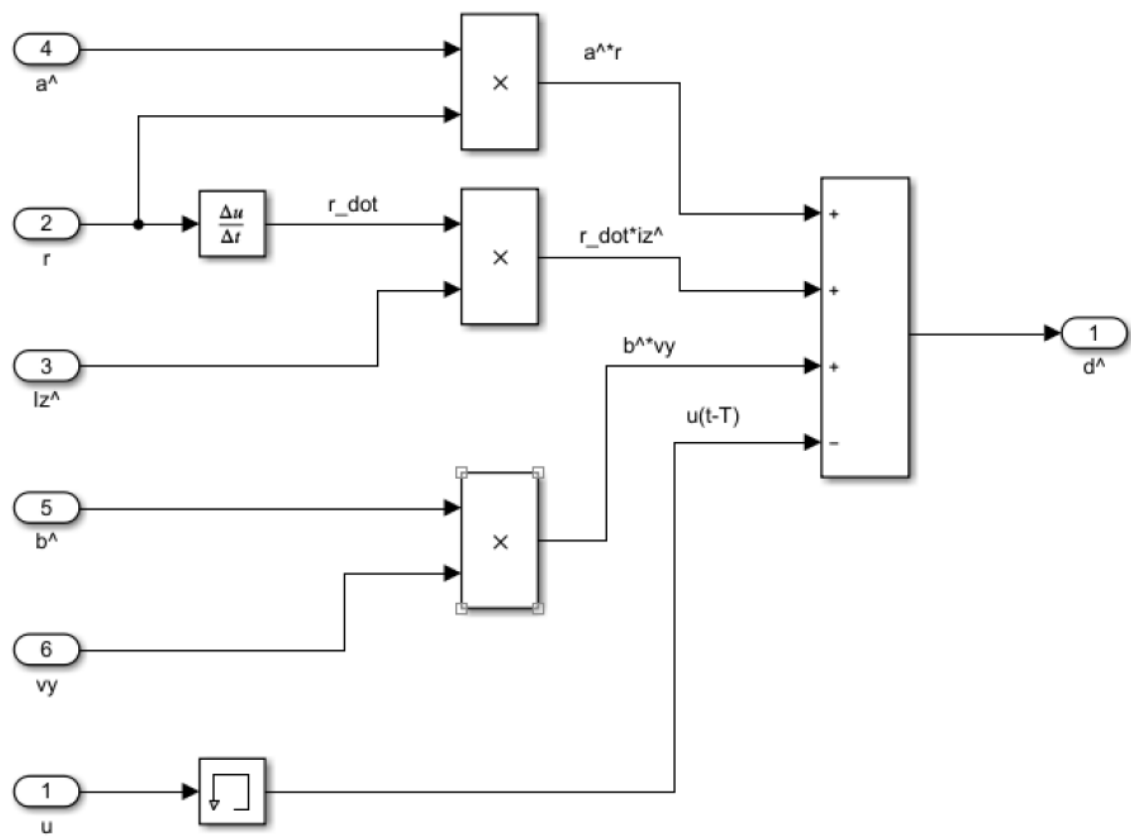


Figure 8: Disturbance estimator subsystem

Chapter 4: Model Predictive Control

4.1: Introduction to Model Predictive Control

Model predictive control (MPC) is a control strategy in which a model is used to predict the system's future behaviour over a finite time window, called the horizon. Based on these predictions and the current measured/estimated state of the system, the optimal control inputs with respect to a defined control objective and subject to system constraints is computed. The measurement, estimate, and computing procedure is repeated with a shifted horizon after a certain time interval. This is why this approach is also known as receding horizon control (RHC).

We prefer MPCs over traditional PID Controllers for the following reasons:

- MPCs can explicitly consider constraints. In our case it will be extremely useful as we can explicitly mention a constraint for our steering wheel angle.
- Using MPCs, we can handle non-linear systems without needing to linearize the system. Since the dynamics model used by CarSim need not necessarily be linear, this property will be helpful.
- The ability of MPCs to predict the future behaviour of the system over a finite time window.

In varying traffic and road circumstances, AGVs must be able to make decisions at each sampling time. The vehicle must also remain within the boundaries of the road. In order to design the path following controller while capturing all of the dynamics that affect the vehicle reaction given the real-time control requirements and road limits, an MPC technique is used. MPC is proposed to design the path tracking controller for AGVs because of its ability to handle multi-variable problems and explicitly consider hard constraints related to the vehicle dynamics and the environment

The vehicle modelled in Chapter 1 and 2 is discretized using the Euler method as shown below

$$\mathbf{X}(k+1) = \mathbf{X}_k + \Delta T \cdot \mathbf{f}_k(\mathbf{X}_k, \mathbf{u}_k) = \mathbf{f}^{\text{dt}}(\mathbf{X}_k, \mathbf{u}_k) \quad (23)$$

where ΔT is the sampling time.

Given the current state X_0 at the current time step t , MPC computes the optimal control sequence u_k with the receding horizon principle, which solves the following optimization problem:

$$\begin{aligned} &\text{Minimise } J_{\text{mpc}}([X_k]^N_k, [u_k]) \\ &\text{Subject to: } X_{k+1} - f^{\text{dt}}(X_k, u_k) = 0 \\ &\quad |u_k| - u_{\text{sat}} \leq 0 \end{aligned} \tag{24}$$

where $k = 0, 1, \dots, N$; N is the prediction horizon, k is the time step within the prediction horizon and u_{sat} denotes the maximum allowable magnitude value of control input. J_{mpc} is the cost function. This cost function is taken care by MATLAB-Simulink while designing the MPC.

4.2: Implementation

The MATLAB-Simulink implementation of the MPC is given below in figure 9. While tuning the MPC, the following values are chosen: prediction horizon = 10, control horizon = 3. The controller consists of two main parts: the MPC and the steering controller. The steering subsystem consists of a closed loop controller with $K_p = 2$ and the transfer function of the steering actuator modelled in (18). The vehicle dynamics are modelled based on bicycle model and is represented in state space. The vehicle is tested for a heading angle change of 10° .

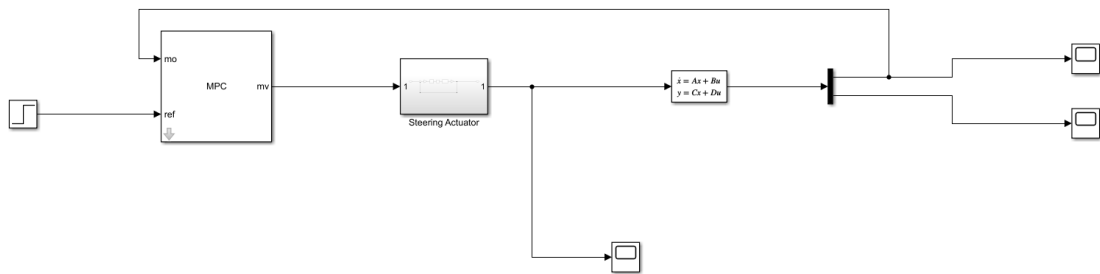


Figure 9: Model Predictive Controller

Chapter 5: Results

The effectiveness of Robust Adaptive Sliding Mode Controller and Model Predictive Controller are evaluated. The tests are conducted for a heading angle change of 10° .

At 5 m/s:

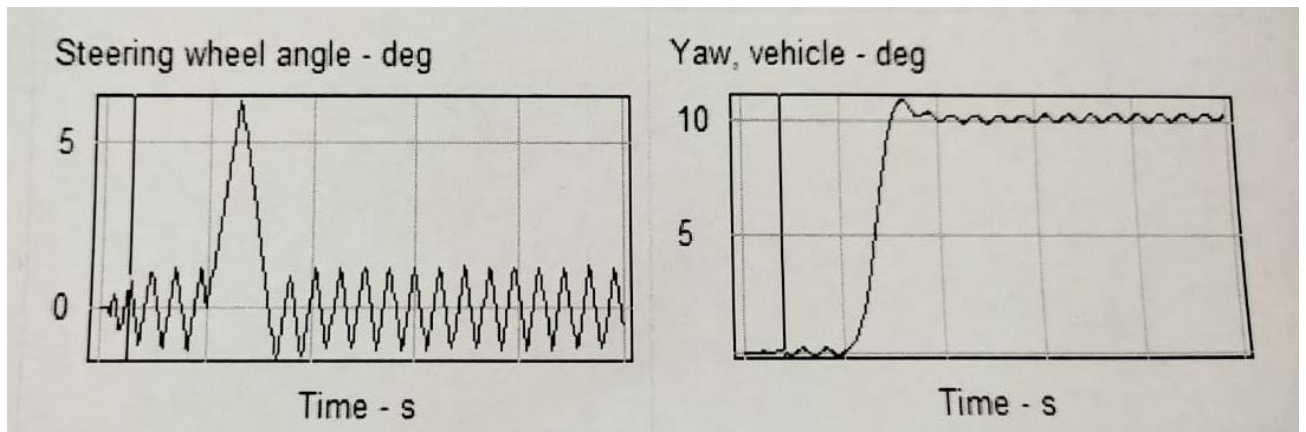


Figure 10: Steering Wheel Angle and Yaw of the AGV at 5m/s with RASMC

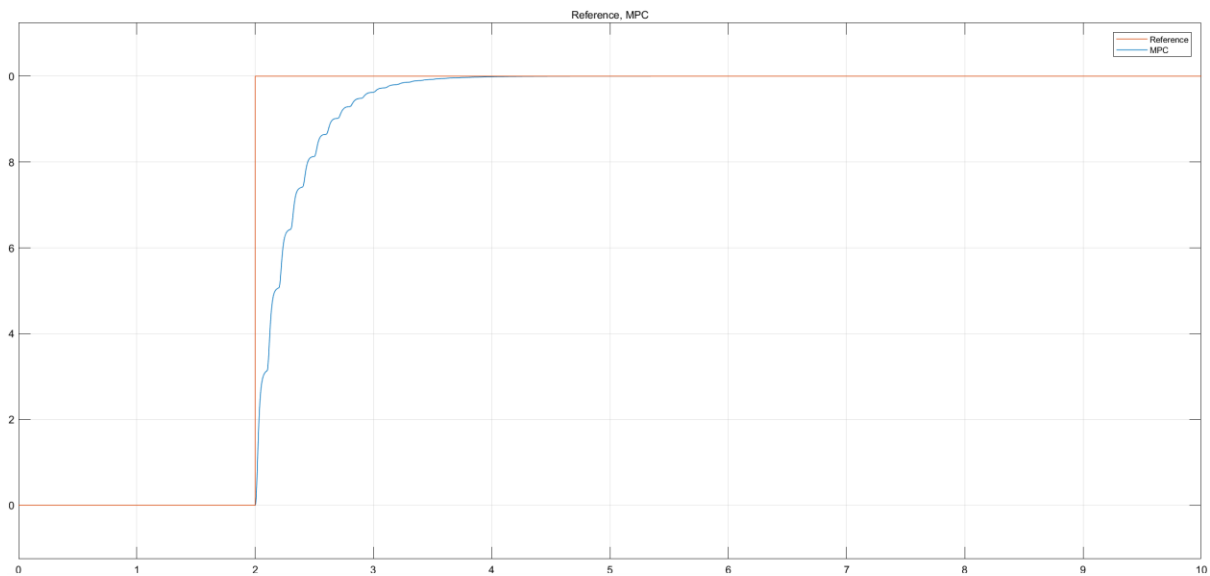


Figure 11: Yaw of the AGV at 5 m/s with MPC

At 10 m/s:

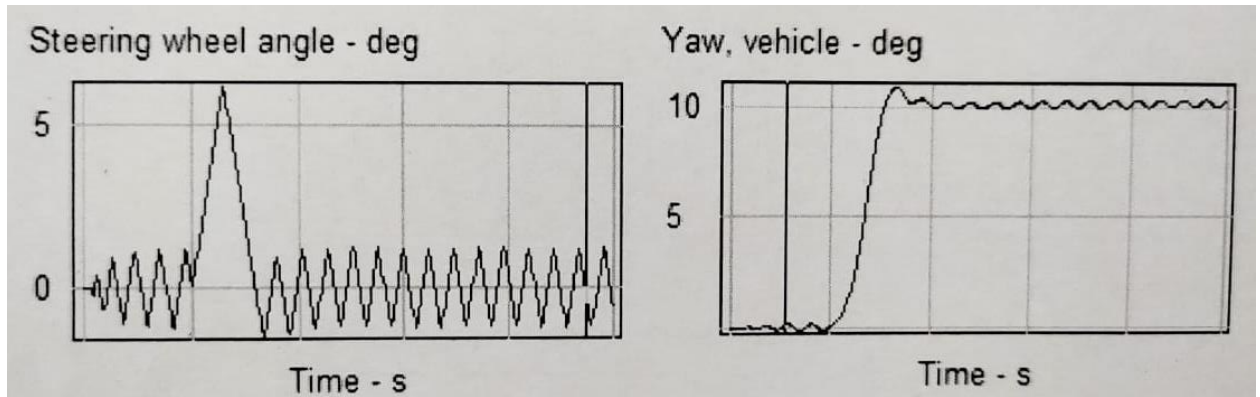


Figure 12: Steering Wheel Angle and Yaw of the AGV at 10 m/s with RASMC

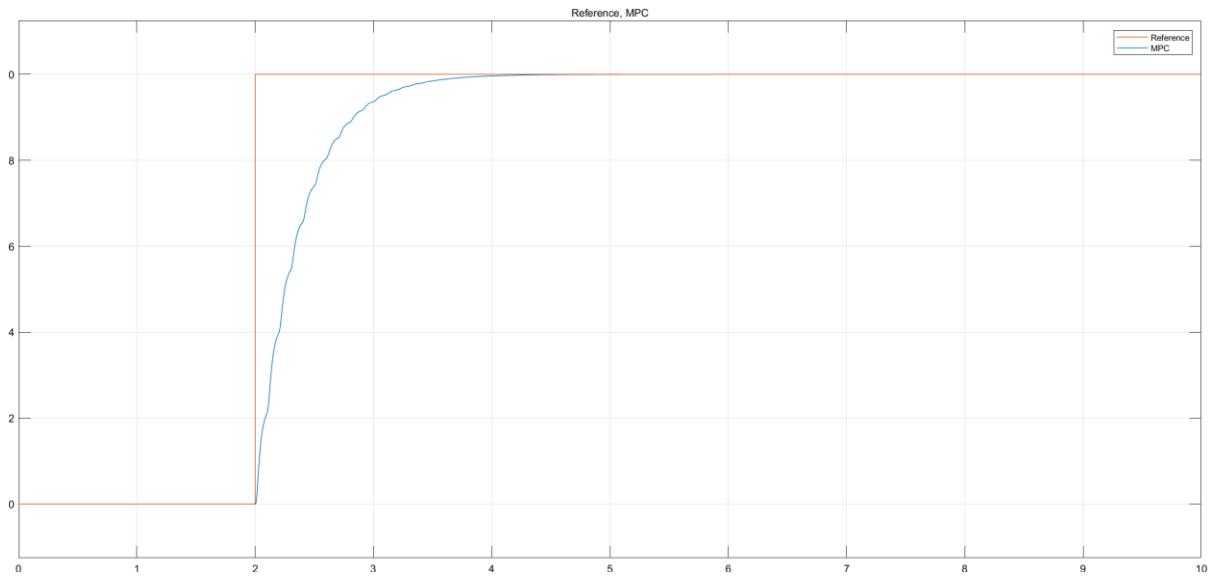


Figure 13: Yaw of the AGV at 10 m/s with MPC

It is observed that upon simulation in MATLAB-Simulink, the MPC is able to achieve a heading angle change of 10° in 2 seconds. Further tests can be done in CarSim to test the effectiveness of the controller. In case of Robust Adaptive Sliding Mode Controller (RASMC) was able to achieve a heading angle change of 10° within 2 seconds in CarSim.

In conclusion, both Robust Adaptive Sliding Mode Controller (RASMC) and Model Predictive Controller (MPC) provide similar and satisfactory results at low speeds. The advantage of MPC over RASMC is that the constraints can be explicitly given in MPC.

References

- [1] T. Morita, H. Takahashi, J. Satonobu, K. Kojima and Y. Morimoto, “An approach to the intelligent vehicle,” in Proc. Intell. Veh. Symp., Tokyo, Japan, pp. 426–431, Jul. 1993
- [2] H. Gharavi, K. V. Prasad, and P. Ioannou, “Scanning advanced automobile technology,” in Proc. IEEE, vol. 95, no. 2, pp. 328–333, Feb. 2007
- [3] Z. Sun, “An intelligent control system for autonomous land vehicle,” Ph.D. dissertation, Dept. Control Eng., Nat. Univ. Def. Technol., Beijing, China, 2004
- [4] Q. J. Han and S. J. Liu, “Path tracking of tracked vehicle,” Int. J. Comput. Sci. Issues, vol. 10, no. 6, pp. 2938–2943, 2013
- [5] N. H. Amer et al., “Adaptive modified stanley controller with fuzzy supervisory system for trajectory tracking of an autonomous armoured vehicle,” Robot. Auton. Syst., vol. 105, no. 2018, pp. 94–111, 2018
- [6] D. Soudbakhsh and A. Eskandarian, “Comparison of linear and non-linear controllers for active steering of vehicles in evasive maneuvers,” Proc. Inst. Mech. Eng., Part I, J. Syst. Control Eng., vol. 226, no. 2, pp. 215–232, 2011
- [7] Z. Sun, J. Zheng, Z. Man, M. Fu and R. Lu., “Nested adaptive super-twisting sliding mode control design for a vehicle steer-by-wire system,” Mech. Syst. Sig. Process., vol. 122, no. 2019, pp. 658–672, 2019
- [8] S. Lv, N. Wang, Y. Wang, J. Yin, M.J. Er., “Nonsingular terminal sliding mode based trajectory tracking control of an autonomous surface vehicle with finite-time convergence,” in Proc. Int. Symp. Neural Netw., pp. 83–92, 2017
- [9] X. Wang and S. Li, “Finite-time trajectory tracking control of underactuated autonomous surface vessels based on non-singular terminal sliding mode,” Aust. J. Elect. Electron. Eng., vol. 9, no. 3, pp. 235–246, 2012
- [10] D. Hrovat, S.D. Cairano, H.E. Tseng, I.V. Kolmanovsky, “The development of Model Predictive Control in automotive industry: A survey”, IEEE International Conference on Control Applications, pp. 295 – 302, 2012
- [11] X. J. Zhao, H. O. Liu, Y. Jiang, and H. Y. Chen, “Backstepping adaptive sliding mode control for automatic steering of intelligent vehicles,” Advanced Science Letters, vol. 6, no. 1, pp. 696–701, 2012.
- [12] H. Yoshida, S. Shinohara, and M. Nagai, “Lane change steering maneuver using

model predictive control theory,” *Veh. Syst. Dyn.*, vol. 46, suppl. 1, pp. 669–681, 2008.

- [13] P. Falcon, F. Borrelli, J. Asgari, H. E. Tseng and D. Hrovat, “Predictive active steering control for autonomous vehicle system,” *IEEE Trans. Cont. Syst. Technol.*, vol. 15, no. 3, pp. 566–580, May 2007.
- [14] Y. Yoon, J. Shin, H.J. Kim., Y. Park, S. Sastry, “Model-predictive active steering and obstacle avoidance for autonomous ground vehicles”, *Control Engineering Practice*, pp. 741-750, 2017
- [15] M. Choi, S.B. Choi, “Model Predictive Control for Vehicle Yaw Stability With Practical Concerns”, *IEEE Transactions on Vehicular Technology*. 63(8):3539 – 3548, 2014
- [16] R. Yu, H. Guo, Z. Sun and H. Chen, "MPC-Based Regional Path Tracking Controller Design for Autonomous Ground Vehicles," 2015 IEEE International Conference on Systems, Man, and Cybernetics, pp. 2510-2515, 2015
- [17] Jazar RN. *Vehicle dynamics: theory and application*. New York: Springer; 2014
- [18] S. Sahoo, S. C. Subramanian and S. Srivastava, "Design and implementation of a controller for navigating an autonomous ground vehicle," 2012 2nd International Conference on Power, Control and Embedded Systems, pp. 1-6, 2012
- [19] S. Sahoo, S.C. Subramanian and S. Srivastava "Sensitivity Analysis of Vehicle Parameters for Heading Angle Control of an Unmanned Ground Vehicle.", *Proceedings of the ASME 2014 International Mechanical Engineering Congress and Exposition. Volume 12: Transportation Systems*. Montreal, Quebec, Canada. November 14–20, 2014
- [20] V. Utkin, "Variable structure systems with sliding modes," in *IEEE Transactions on Automatic Control*, vol. 22, no. 2, pp. 212-222, April 1977